Complex Living Materials Made by Light-Based Printing of Genetically Programmed Bacteria

Originally published in:
Advanced Materials 35(6), https://doi.org/10.1002/adma.202207483

ADVANCED MATERIALS
www.advmat.de

Complex Living Materials Made by Light-Based Printing of Genetically Programmed Bacteria

*Marco R. Binelli, Anton Kan, Luis E. A. Rozas, Giovanni Pisaturo, Namita Prakash, and André R. Studart**

Living materials with embedded microorganisms can genetically encode attractive sensing, self-repairing, and responsive functionalities for applications in medicine, robotics, and infrastructure. While the synthetic toolbox for genetically engineering bacteria continues to expand, technologies to shape bacteria-laden living materials into complex 3D geometries are still rather limited. Here, it is shown that bacteria-laden hydrogels can be shaped into living materials with unusual architectures and functionalities using readily available light-based printing techniques. Bioluminescent and melanin-producing bacteria are used to create complex materials with autonomous chemical-sensing capabilities by harnessing the metabolic activity of wild-type and engineered microorganisms. The shaping freedom offered by printing technologies and the rich biochemical diversity available in bacteria provides ample design space for the creation and exploration of complex living materials with programmable functionalities for a broad range of applications.

1. Introduction

Exploiting microorganisms to fabricate engineered living materials is an enticing strategy to imbue synthetic materials with self-healing, regenerating, responsive, and adaptive properties using sustainable biological processes.[1,2–4] In the field of building materials, alkaline-resistant bacteria have been used to fix structural damage through local mineralization processes, leading to self-healing concrete with enhanced corrosion resistance, fracture toughness, and regeneration capabilities.[5] In addition to bacteria-induced mineralization, the direct growth of fiber-like mycelia by fungi have also been exploited to create self-regenerating living skins for robotic applications.[6] Moreover, a variety of bacterial species have been engineered to create living materials for catalysis, energy conversion, sensing, and electronic applications.[7] In the biomedical area, therapeutic hydrogels have been developed by genetically programming *E. coli* to secrete modified curli fibers that selectively interact with the tissue of the gastrointestinal tract.[2] Using optogenetic approaches, *E. coli* have also been engineered to enable the light-induced secretion of adhesive proteins that promote the attachment of mammalian cells on hydrogel surfaces.[4] These examples illustrate the great potential of microorganisms in extending the functionalities of engineering materials in a broad range of applications.

The programmable and versatile biological machinery of microorganisms, in particular bacteria, is key to cover a wide spectrum of engineering-relevant functionalities. Indeed, bacteria have evolved rich and versatile biochemical networks, which can be engineered and deployed at large scales due to their smaller genomes and faster growth rates. Moreover, the presence of a cell wall makes bacteria mechanically and chemically robust to survive even in harsh environments. While these features have allowed prokaryotes to dominate the Earth for 2 billions of years and to form intricate biofilm structures,[8] more complex 3D morphologies of bacteria often rely on symbiosis of these microorganisms with host animals and plants. Such morphological limitation has prevented prokaryotes from reaching the size and level of complexity found in tissues made by eukaryotic cells. Clearly, complex morphology and multiscale architecture are crucial for the performance and function of animal and plant tissues in the natural world.[9] In this context, combining the rich biochemistry and robustness of bacteria with the complex shapes of eukaryotic tissues is expected to open many new opportunities in the field of engineered living materials.

Materials with complex multiscale architectures can be effectively manufactured using 3D printing techniques.[10] Current printing methods, including extrusion- and light-based approaches, enable the fabrication of complex-shaped materials using a variety of feedstock inks. By designing the building blocks of the ink, hierarchical materials with intricate architectures have been made out of ceramics, metals, polymers, and composites. Inks loaded with human cells have also been used to print artificial tissues for biomedical applications.[11] While printing technologies for organs and tissues continue to advance, the focus of this research has been primarily on human-relevant eukaryotic cells for tissue regeneration and drug discovery. To harness the potential of microorganisms in

M. R. Binelli, A. Kan, L. E. A. Rozas, G. Pisaturo, N. Prakash, A. R. Studart
Complex Materials
Department of Materials
ETH Zürich
Vladimir-Prelog-Weg 5, Zürich 8093, Switzerland
E-mail: andre.studart@mat.ethz.ch

The ORCID identification number(s) for the author(s) of this article can be found under https://doi.org/10.1002/adma.202207483.

DOI: 10.1002/adma.202207483

engineered living materials, hydrogels containing bacteria have been successfully printed using the extrusion-based direct ink writing approach.[3,12,13] The main advantage of this technique is the ability to create multimaterial structures with spatially controlled arrangement of different bacteria. However, extrusion-based techniques cannot reach the level of shape complexity and spatial resolution enabled by light-based printing methods.[14] Printing programmable bacteria using light is therefore expected to significantly broaden the design space of engineered living materials toward more complex architectures and functionalities.

Here, we demonstrate a manufacturing platform for the shaping of bacteria-laden hydrogels into living materials with complex geometries and programmable functionalities using state-of-the-art light-based printing technologies. To ensure cell viability and high-resolution printing, we first design and characterize biocompatible hydrogels with well-defined rheological properties and rapid photoactive response. The selected photoactive hydrogel is then embedded with wild-type bioluminescent bacteria to create light-emitting living objects with unique complex morphology and enhanced luminescence. Microorganisms engineered to secrete melanin in response to a specific chemical were also incorporated in the hydrogel to generate another living ink. We finally demonstrate the unique capabilities of the printing platform by combining the two inks to create a functional living device with a multibacteria architecture that enables self-powered chemical sensing through a simple visual cue.

2. Results and Discussion

Complex living hydrogels are created by 3D-printing aqueous solutions loaded with wild-type or genetically engineered bacteria (**Figure 1**). Two types of bacteria were selected to demonstrate how the biological machinery of selected and engineered microorganisms can be harnessed to produce a functional living material. Because of their direct visual effect, we design and print hydrogels that contain bacteria that are able to either emit light or block the transmission of light through the structure. The bioluminescent bacteria *Photobacterium kishitanii*, a bright and robust strain extracted from deep-sea fish,[15] are embedded in the hydrogel to emit light in the blue-green range of the visible spectrum. To block light, we genetically engineer *E. coli* to produce light-absorbing melanin particles through an enzymatic reaction in response to a specific chemical trigger. These microorganisms are incorporated in the photoactive solution individually or combined to create complex-shaped objects with color-changing behavior. When combined in a single living object, the interplay between the bacteria under different chemical environments controls the color of the printed hydrogels over time.

The intricate geometry of the envisioned object is generated using either digital light processing (DLP) or volumetric printing (VP) as light-based additive manufacturing approaches. DLP is a layer-by-layer process that is most suitable to print complex-shaped objects with high resolution out of a single ink.[16] VP is a manufacturing tool that complements DLP technologies by enabling the creation of macroscopic objects at high throughputs and with multiple material compositions.[17,18] We use DLP to study the effect of geometry on the bioluminescent behavior of bacteria-laden objects, whereas VP is utilized to create multimaterial living structures containing both *P. kishitanii* and engineered *E. coli*. Because DLP and VP require fluids with distinct rheological behavior, the composition of the cell-laden ink was optimized to reach flow properties that still lie within the boundaries of these two printing techniques.

Light-based 3D printing of bacteria-laden complex materials is carried out by formulating an aqueous ink that contains the microorganism of interest suspended in a mixture of photopolymerizable species. To ensure high cell viability, the photopolymerizable mixture contains methacrylated hyaluronic acid (HAMA) and a methacrylated PEO-PPO-PEO copolymer (Pluronic F-127, Plu) as biocompatible multi- and di-functional monomers, respectively (Figure 1c). The methacrylated copolymer, hereafter PluDMA, was synthesized by introducing methacrylate reactive groups at the ends of the PEO-PPO-PEO copolymer chain (Figure S1, Supporting Information).[12] Besides the monomers above, quinoline yellow is utilized as a dye to control the light penetration depth and lithium phenyl-2,4,6-trimethylbenzoylphosphinate (LAP) is used as biocompatible photoinitiator.

To print bacteria-laden hydrogels with complex geometries, the DLP ink needs to be fluid enough to easily flow under the printhead but also sufficiently strong upon polymerization to enable the manufacturing of mechanically stable high-resolution objects. The PluDMA copolymer present in the DLP ink is deliberately designed to fulfill these requirements. By providing reactive methacrylate groups at both ends of its chain, PluDMA forms a highly cross-linked network with HAMA after photopolymerization, while keeping the initial ink sufficiently fluid to effectively replenish the printing tray during the DLP process. Printing experiments of model pillar structures reveal that formulations with PluDMA allow for the manufacturing of distortion-free objects (Figure 1d) with dimensional deviation below 18% of nominal values for printed feature sizes up to 1 mm and below 7% for feature sizes up to 1 cm (Figure 1e).

Further insights into the role of PluDMA in the printing process are gained by measuring the rheological behavior of inks containing 20% w/v of this molecule compared to control formulations. In these measurements, the viscoelasticity of the ink was quantified using oscillatory rheology, whereas steady-state shearing tests probed the apparent viscosity of the formulation. The oscillatory tests reveal that the inks are fluids with no noticeable yield stress, which enables gravity-induced flow of the feedstock under the printhead (Figure S2, Supporting Information). The steady-state flow measurements indicate that all inks exhibit shear-thinning behavior when subjected to shear rates up to 100 s^{-1} (Figure 1f). The presence of an additional 20% w/v of Plu or PluDMA was found to increase the zero-shear viscosity (η_0) of the HAMA inks by a factor of 10. Importantly, the (η_0) value of 23.40 Pa s measured for the PluDMA-containing ink is sufficiently low to allow for quick flow under the effect of gravity.

In addition to the initial flow properties, rheological tests were also performed to evaluate the stiffening of the inks during the light-induced polymerization process. To this end,

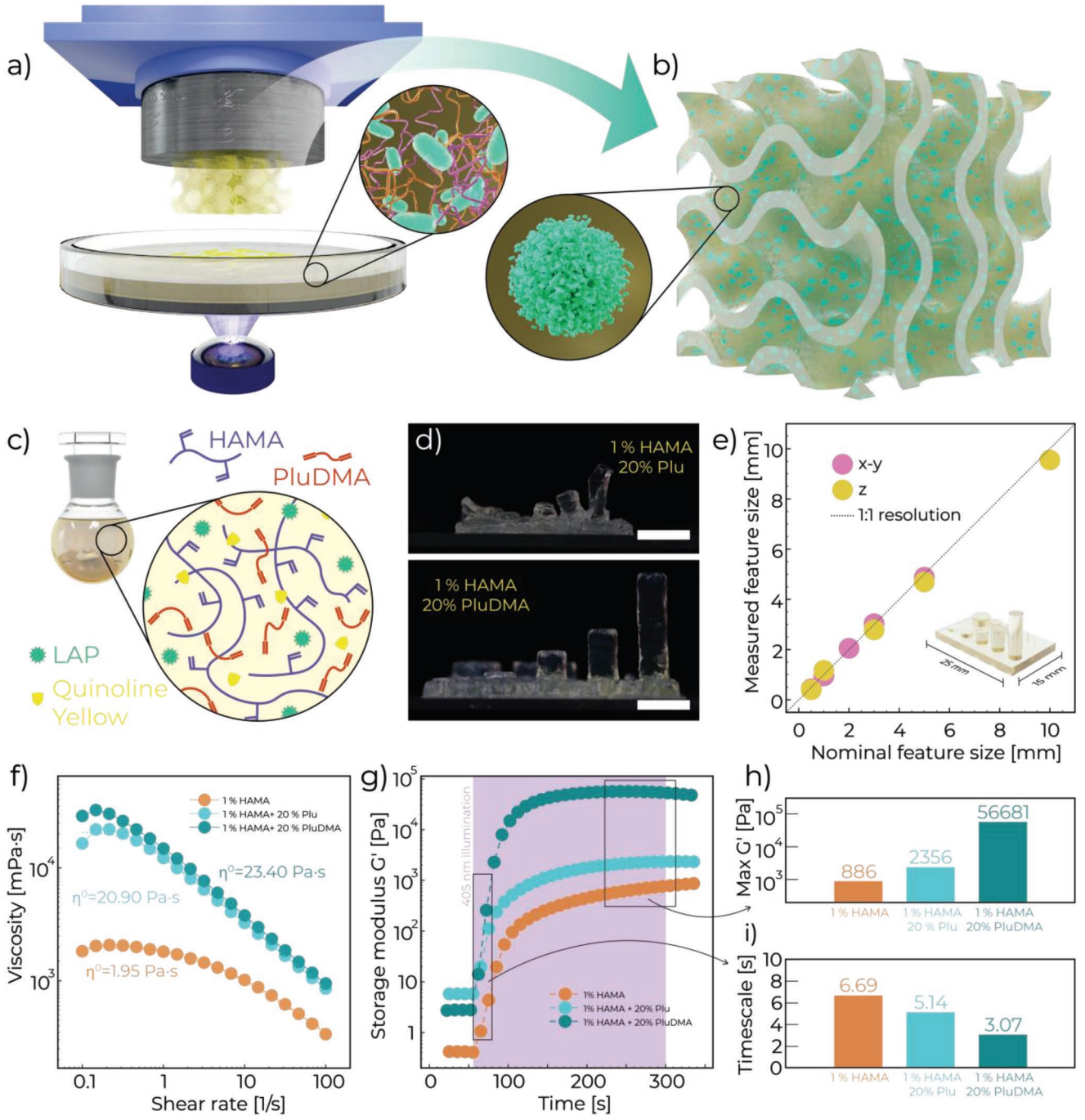

Figure 1. Printing technology and hydrogel inks used for shaping complex living materials. a) Schematics of a DLP setup employed to print bacteria-laden hydrogels. b) Cartoon of a printed living material with gyroid structure, highlighting the typical globular colonies of bacteria formed after immersion in culture medium. c) Schematics displaying the composition of the photocurable ink, which typically contains HAMA, a PEO-PPO-PEO copolymer (Pluronic F-127) in its unmodified (Plu) or dimethacrylated forms (PluDMA), a photoinitiator (LAP), and a dye (quinoline yellow). d) Photographs of test plates printed by DLP to assess the spatial resolution and geometrical accuracy achieved with distinct ink formulations. Plates printed with inks containing unmodified (Plu) and dimethacrylated (PluDMA) copolymer are shown in the top and bottom images, respectively. Scale bar: 5 mm. e) Printing fidelity obtained within the printing plane and along the normal printing direction using the HAMA-PluDMA ink. The dashed line indicates the condition for 1:1 printing fidelity, which corresponds to an exact match between the size of the digital file and of the print. Measurements were conducted on three samples per point. The error bars are within the size of the symbols. f) Apparent viscosity as a function of the applied shear rate for distinct ink formulations. g) Time evolution of the storage modulus of different ink compositions upon illumination with light at wavelength of 405 nm. Representative runs are displayed in graphs (f,g) to showcase the outcome of each experimental condition. h) Maximum storage modulus and i) characteristic timescale for polymerization of the investigated hydrogel inks.

we measured the evolution of the storage modulus of selected formulations upon illumination with a 405 nm light-emitting diode (LED) while imposing a low-amplitude oscillatory stress on the sample (Figure 1g). The results show that the light-induced polymerization increases the storage modulus of the sample by several orders of magnitude, reaching values of 886, 2356, and 56 681 Pa, for the HAMA, HAMA-Plu, and HAMA-PluDMA formulations, respectively (Figure 1g). The tenfold higher storage modulus obtained in the presence of PluDMA reflects the high cross-linking density achieved with the modified copolymer and explains the high mechanical stability and resolution of objects printed with this formulation (Figure 1h,d). Moreover, the increased concentration of reactive methacrylates present in the HAMA-PluDMA ink reduces by approximately twofold the cross-linking timescale (Figure 1i). This is due to the shorter diffusion jumps necessary for the radicals generated during illumination to reach a methacrylate moiety. The timescale of 3 s measured for the HAMA-PluDMA formulation closely matches the illumination timescale for DLP printing, confirming the suitability of the ink for the process.

The biocompatibility, rheological properties, and photoactive response of PluDMA-containing inks make them highly suitable for the light-based printing of strong hydrogels with embedded microorganisms. Microorganisms are incorporated into the aqueous photo-active mixture by simply inoculating the ink with the bacteria of interest. To prevent chemical incompatibilities with the reactive monomers, the salts and biomolecules typically used in the cell culture medium are not added to the initial bacteria-laden ink. We found that bacteria are generally robust enough to remain alive in the ink for hours without nutrients. This allows for printing of complex objects that can be later immersed in culture medium to promote bacterial growth and activate the biological machinery needed to achieve the envisioned function.

To generate luminescence in our printed objects, we exploited the native biological machinery of *P. kishitanii*. Bioluminescence in these marine bacteria relies on the expression of the luciferase enzyme complex, which enables the emission of blue-green around 490 nm in wavelength through the oxidation of two substrates, namely, a long-chain aliphatic aldehyde and reduced flavin mononucleotide (**Figure 2**a).[19] The luciferase genes are encoded in the genome and expressed in an operon containing several *lux* genes, the *luxCDABFEG* operon (Figure 2a). The luciferase enzyme itself is made up of two subunits, *luxA* and *luxB*, whereas the remaining genes encode enzymes used in substrate synthesis, namely, a fatty-acid reductase complex (*luxCDE*) and a flavin reductase (*luxG*). Here, the bioluminescent properties of *P. kishitanii* were first evaluated by measuring the light emitted by bacteria grown in liquid culture. The obtained spectra show a broad intensity peak centered around 480 nm, which corresponds to a vivid blue-green color. The luminescence of the culture was dependent on cell density as well as the growth phase of *P. kishitanii* in the culture medium (Figure 2b), with the highest bioluminescence rates present during the exponential phase (Figure 2c).

To evaluate whether *P. kishitanii* can still grow and luminesce when entrapped in the cross-linked hydrogel, we polymerized bacteria-laden inks and optically imaged the obtained samples after the photo-curing process (Figure 2d). Samples were prepared using inks inoculated with a bacteria suspension that was pre-cultured for 12 h to reach a high initial concentration of cells in the cross-linked gel. The resulting polymerized samples were then immersed in culture medium and imaged at increasing time intervals using bright-field optical microscopy. Snapshots of the samples reveal that the micron-sized bacteria grow into well-defined colonies, which continuously increase in size from 30 to 384 μm^2 before reaching a plateau after 72 h of incubation (Figure 2d,e). The formation of such spatially resolved colonies probably results from the confined environment provided by the viscoelastic gel.[20] When imaged under dark conditions, the colonies emit a bright luminescence that is readily visible by the naked eye (Figure 2f,g and Figure S3, Supporting Information). The observed growth and bioluminescence indicate that the bacteria remain functional and metabolically active even when entrapped in the hydrogel.

The ability to maintain the bacteria metabolically active inside the printed hydrogel opens the possibility to design and create functional macroscopic objects with living morphologies that are not found in the natural world. We illustrate this by printing the bacteria-laden hydrogel into a complex-shaped gyroid structure (Figure 2g and Figure S3, Supporting Information). Because of its bi-continuous periodic minimal surface,[21] the gyroid geometry displays an open channel network that facilitates the transport of fluids into the structure while keeping a high mechanical stability.[22] In our experimental demonstration, we harness these geometry-specific features to enhance the supply of nutrients and removal of waste from the bacteria embedded in the hydrogels, which is expected to increase the bacterial density and the luminescence of the printed object.

The bioluminescence of bacteria-laden hydrogels with a gyroid structure was then compared with that of cubic objects of equivalent bounding volume. The unique architecture of gyroids was reproduced with high fidelity in the printed hydrogels, confirming the high resolution and mechanical stability provided by the PluDMA-containing ink. The specific luminescence of the bacteria-laden hydrogels over the course of 6 days was found to be stronger by up to two orders of magnitude as compared to the cubic sample immersed in the same culture medium (Figure 2f). The samples showed increasing luminescence until 3–4 days of culture, after which the bioluminescence intensity started to drop. The time needed to reach maximum luminescence matches reasonably well with the time corresponding to the plateau in bacterial growth (Figure 2d), suggesting that the bioluminescence of the printed objects reflects the density of bacteria embedded in the hydrogel.

While the luminescence function relies on the native machinery of the wild-type *P. kishitanii*, we opted to control light transmission through the material by the on-demand synthesis of melanin pigment in a strain of *E. coli*. Synthesis of melanin by *E. coli* is made possible by genetically engineering the bacteria to produce the enzyme tyrosinase. This copper-containing enzyme is present in bacteria, as well as animal, fungal, and plant tissue, where it is used for the production of the dark pigment melanin through the oxidation of phenols, such as tyrosine.[23] If the substrate tyrosine is supplied to the culture medium, the tyrosinase molecules displayed on the surface of the engineered bacteria are expected to catalyze the polymerization reaction leading to the synthesis of melanin (**Figure 3**a,b). To perform the envisioned chemical sensing function, the synthesis of melanin by *E. coli* was programmed

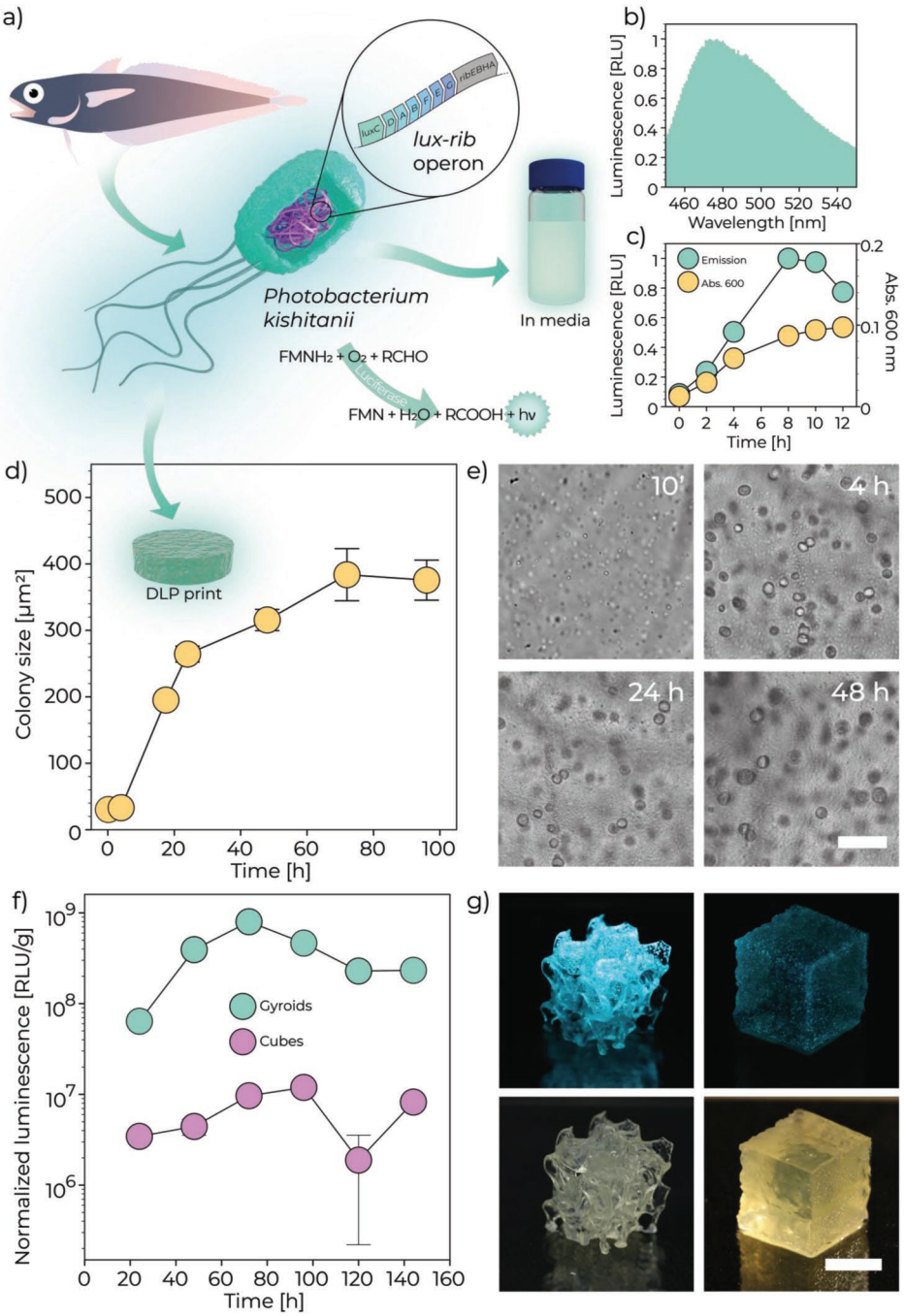

Figure 2. Printed hydrogels containing bioluminescent bacteria. a) *P. kishitanii* are gram-negative, coccoid-rod, motile bacteria found in the light organ of *Physiculus japonicus*, a deep-sea fish living in the waters of Japan. The strain displays intense cyan luminescence because of the presence of the *lux* genes, which *P. kishitanii* exhibits in the *lux-rib* operon found on the genome (see inset). b) Light emission spectrum of a liquid culture of *P. kishitanii*, displaying an intensity peak around 475 nm. c) Evolution of the optical density at 600 nm (OD 600) and luminescence of a liquid culture of growing *P. kishitanii*. d) Evolution of the size of bacteria colonies formed in printed hydrogels containing *P. kishitanii*. The inset shows the disk-shaped structures printed for imaging. We display the average area of the colonies imaged on a number of identical samples, $n = 3$. The error bars correspond to the standard error of the mean for all the colonies identified at each time point. e) Micrographs of printed bacteria-laden hydrogels taken under bright-field illumination at different time points after printing. Scale bar: 100 µm. f) Normalized luminescence of printed gyroids and cubes measured over 6 days in culture medium. The data points represent averages and the error bars correspond to the standard error of the mean for a number of samples, $n = 3$. g) Photographs of gyroids (left) and cubes (right) printed with hydrogel inks loaded with *P. kishitanii*. The structures are photographed either under illumination (bottom) or in darkness with longer exposure times to capture their bioluminescence (top). Scale bar: 5 mm.

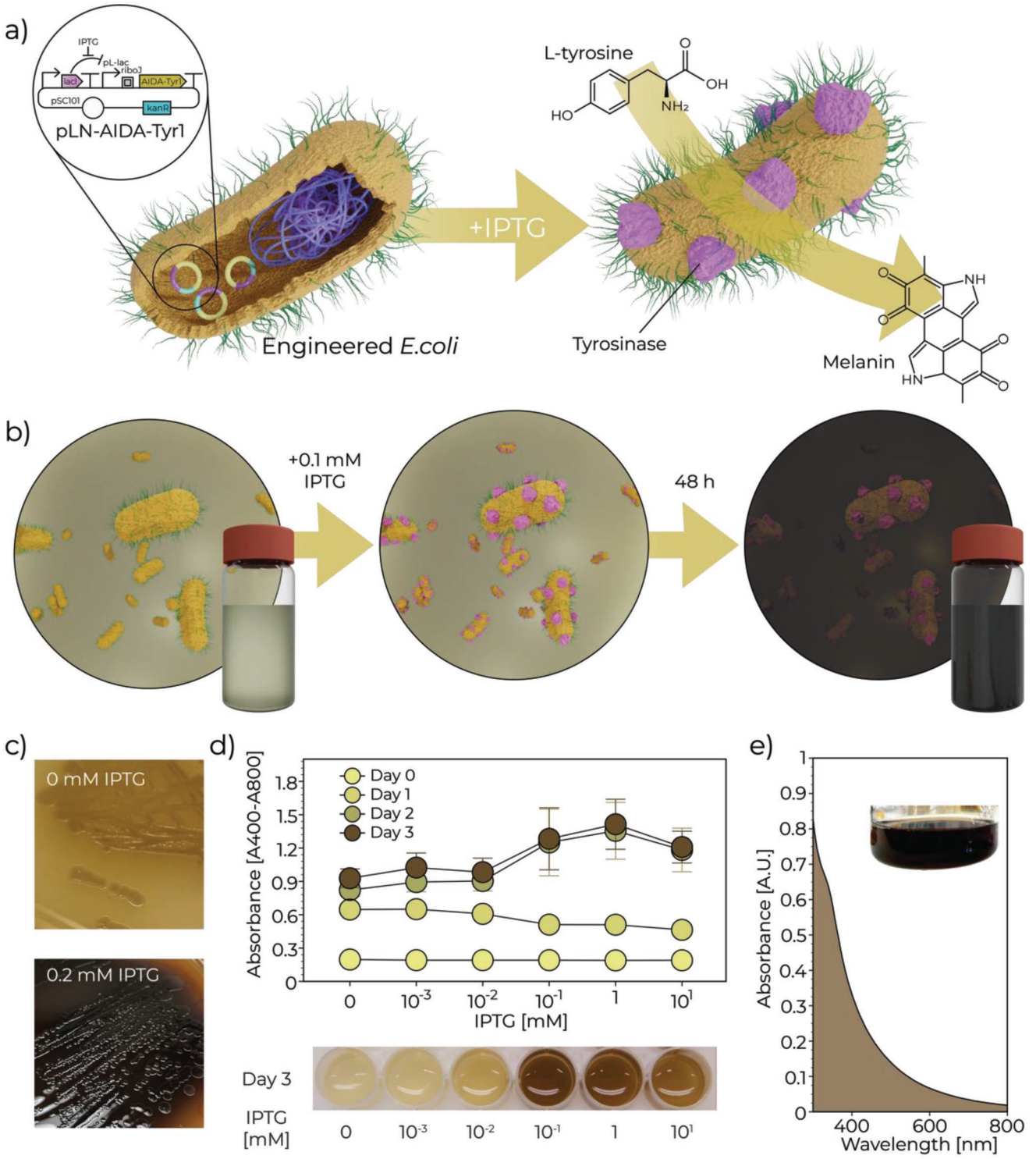

Figure 3. Genetically engineering *E. coli* for the chemically induced production of melanin. a) Cartoon displaying the engineered *E. coli* and the plasmid constructed to express tyrosinase (pLN-AIDA-Tyr1). Upon addition of IPTG, tyrosinase (in pink) is produced and tethered to the external surface of *E. coli*. Tyrosinase catalyzes the oxidation of tyrosine present in the medium, resulting in the extracellular formation of melanin. b) Schematics depicting the effect of the IPTG-induced conversion of tyrosine to melanin on the optical appearance of the bacteria-containing medium. c) Photographs of agar-plated cultures of engineered *E. coli* in the absence and in the presence of IPTG. d) Optical absorbance of agarose-plated cultures prepared with different concentrations of IPTG. e) Absorbance spectrum of the melanin produced by the engineered bacteria collected by washing the plated cultures. The inset shows a photograph of the melanin solution used for the measurement. The data points displayed represent averages with d) $n = 11$ and e) $n = 3$, whereas the error bars in (d) correspond to the standard deviations.

to occur in the presence of a well-known model chemical inducer, namely, isopropyl b-D-1-thiogalactopyranoside (IPTG).

The gene encoding the tyrosinase enzyme (Tyr1) from *Bacillus megaterium* was expressed in translational fusion with an autotransporter protein (AIDA) to enable the expression of the melanin-producing enzyme on the outer surface of the engineered bacteria.[24] AIDA-Tyr1 expression was regulated by the pL-lac promoter,[25] and the LacI repressor was expressed constitutively in a separate transcriptional unit. Therefore, in uninduced conditions, LacI is bound to the promoter and represses transcription, but upon IPTG addition, the repression is lifted and tyrosinase is expressed. To maximize the production of melanin in the *E. coli*, the ribosome binding site (RBS) of the AIDA-Tyr1 fusion was varied to identify optimal mutants, resulting in the final plasmid pLN-AIDA-Tyr1.

To evaluate whether the genetic construct effectively expresses the tyrosinase molecules under chemical stimulus, we plated the transformed *E. coli* onto agar plates with and without IPTG. The darker color of the plate containing 0.2×10^{-3} M IPTG suggests that the synthesis of melanin by the engineered bacteria is promoted by the inducer as expected (Figure 3c). To further validate this interpretation, we performed light absorption measurements on aqueous solutions obtained from washing the dark IPTG-containing agar plates. The experimental data obtained show the typical absorption spectrum of melanin, which is characterized by an increasing absorption as the wavelength is reduced from to 600 to 300 nm (Figure 3e).[26] This confirms that the engineered bacteria can successfully produce melanin in the presence of the chemical inducer.

We then investigated melanin production for *E. coli* cells embedded in a low-melt agarose hydrogel to quantify the effect of the IPTG concentration on the optical absorbance of the plate after 0, 1, 2, and 3 days of incubation in the presence of 1 g L^{-1} tyrosine. In agreement with previous work,[24] our experiments reveal that the production of melanin primarily occurred between day 1 and 2 of incubation (Figure 3d). Moreover, an IPTG concentration of 0.1×10^{-3} M was found to be optimum to maximize the production of melanin. The drop in melanin production observed at higher IPTG concentrations might be related to the possible toxic effect associated with the high expression of AIDA-Tyr1. Importantly, culture experiments showed that the engineered *E. coli* are also able to grow and remain metabolically active in the marine broth used to culture *P. kishitanii*. This opens the way for the 3D printing and co-culturing of the two bacteria species in a single functional living material.

The creation of an exemplary functional living material using the proposed printing platform is illustrated by manufacturing a complex-shaped device that combines bioluminescence and darkening responses programmed within the genetics of the embedded bacteria. The living device is designed to work as a metabolically powered chemical sensor that is able to generate its own light source and detect a specific chemical through a simple visual output. The chemically driven internal light source is provided in the form of bioluminescence through the action of *P. kishitanii*, whereas chemical detection is achieved by the darkening effect resulting from the molecularly induced synthesis of melanin by the engineered *E. coli* (**Figure 4**c). The spatial distribution of the bacteria within the living device is designed such that the bioluminescent *P. kishitanii* is embedded in a core hydrogel, which is covered by another hydrogel layer containing the melanin-producing *E. coli*. In such an architecture, the inner core would be functionally analogous to a light bulb, while the outer layer plays the role of a darkening skin. Because the bioluminescence and darkening effects are chemically powered, the device can function autonomously while it is supplied with the basic constituents of the culture medium.

To manufacture the functional living device, we employ the VP technique using two HAMA-PluDMA inks loaded with either *P. kishitanii* or engineered *E. coli* (Figure 4a and Figure S4, Supporting Information). Multimaterial printing of the dual-bacteria sensor is possible with this technique if the object is manufactured in two sequential steps. First, an ink containing engineered *E. coli* is photopolymerized under 3D projected light to generate the shell (outer layer). The high transparency of the ink is crucial to ensure high fidelity of the printed parts. In a second step, the polymerized shell is washed and re-introduced into a vial containing a second ink loaded with *P. kishitanii*. To restrict the bioluminescent bacteria to the core of the device, it is crucial to position the first printed part at the center of the vial in this second printing process. In contrast to DLP printing, the volumetric approach requires the ink to be sufficiently viscous to inhibit the possible sedimentation of the printed object upon polymerization.[18] With a zero-shear apparent viscosity above 1 Pa s (Figure 1f), the HAMA-PluDMA ink fulfills this rheological requirement.

VP experiments with the HAMA-PluDMA ink were conducted to evaluate the suitability of this manufacturing process in generating the dual-bacteria living device (Figure 4a). Our experiments reveal that complex-shaped objects can be printed in about 10 s at length scales up to a centimeter (Figure 4b). Using HAMA-PluDMA inks, we found that the printed objects do not show the wavy surfaces and the interlayer defects often observed in parts printed with layer-by-layer approaches (Figure 4b). Moreover, VP of HAMA-PluDMA inks loaded with *P. kishitanii* led to objects with uniform luminescence after immersion in culture media for 1 day (Figure 4b). Following the two-step manufacturing protocol, a vase-shaped shell laden with engineered *E. coli* was successfully filled with a hydrogel loaded with *P. kishitanii*. Since the same formulation is used for both inks, the outer shell is closely bound to the inner core at the end of printing process. Such strong adhesion prevented delamination between the inner and outer hydrogels for the whole duration of the study. Detachment only occurred in samples maintained in culture for several weeks, which is likely a result of mechanical stresses arising from shaking and handling. The final living object illustrates how multimaterial printing of bacteria-laden inks can enable the co-culture of microorganisms with designed complex morphologies.

The use of the co-cultured printed object as a chemical sensor was assessed by measuring the bioluminescence and the light absorption of the living material during culture for up to 7 days (Figure 4d–f). In this experiment, both the bioluminescence and the light absorption of the devices were quantified using a plate reader and the color change was

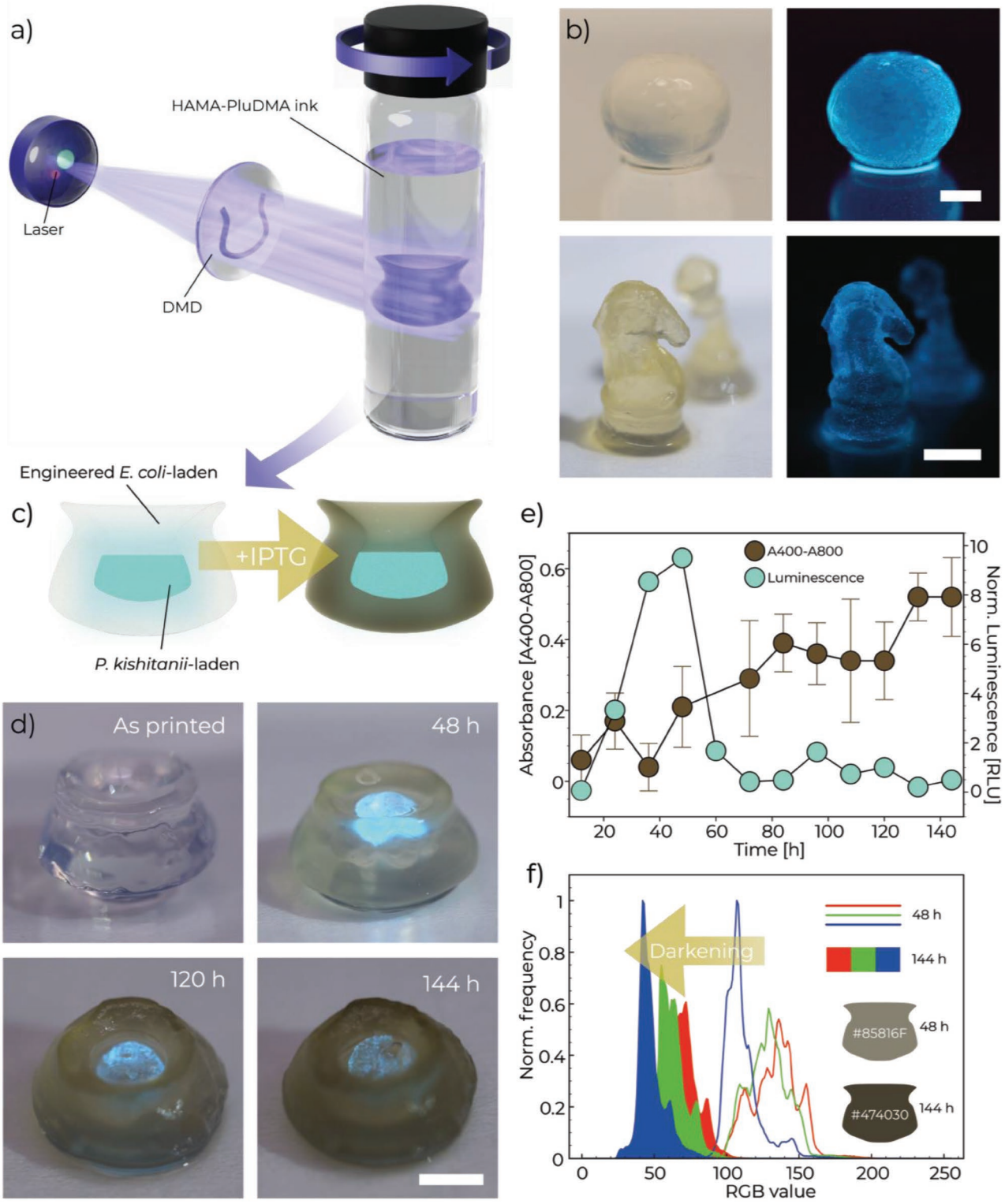

Figure 4. Fabrication and characterization of living multimaterial devices. a) Cartoon displaying the working principle of VP. b) Photographs of a sphere (top) and two chess pieces (bottom) printed with a *P. kishitanii*-laden ink using VP. The pictures on the right were taken in a dark room with longer exposure times to observe the bioluminescence of the structures. Scale bars: 2 mm (top) and 5 mm (bottom). c) Schematics of the working principle of the printed multimaterial living device. d) Overlaid photographs of the printed device showing the precise localization of both bacterial strains and the evolution of the outer color and bioluminescence over time. Scale bar: 5 mm. e) Evolution of bioluminescence and absorbance of the printed devices over the course of a week. The points of the absorbance data represent averages and the error bars correspond to the standard error of the mean for a number of samples, $n = 3$. The bioluminescence data shown are from a representative sample. f) Normalized RGB spectra obtained from photographs of the devices after 48 and 144 h. Inset: the corresponding HEX colors resulting from the spectra.

extracted directly from images. Melanin production by the *E. coli* embedded in the outer shell of the object was induced at the beginning of the experiment by adding 0.1×10^{-3} M IPTG as a model chemical to tyrosine- and $CuSO_4$-enriched culture media. The media were periodically replaced every day for the entire duration of the experiment. Our results show that over the course of a week the printed structures exhibited a measurable darkening because of the conversion of tyrosine to melanin. Both the absorbance of the shells (Figure 4e) and their visible color (Figure 4f) gradually changed, while the cores were still emitting light up to the last day (Figure 4d). As a consequence of the darkening of the shell, the luminescence detectable by the plate reader also visibly dropped, thereby providing a straightforward readout for the presence of IPTG. To further characterize the sensing capacity of the material, we performed experiments with disk-shaped devices, finding that the addition of IPTG led to the material darkening and reduced the transmitted luminescence (Figure S6, Supporting Information). A statistically significant difference was observed for the absorption data in the presence of IPTG relative to control samples, whereas further experiments are required to reach statistically relevant values for the luminescence data. Overall, we were able to fabricate complex structures with two different strains of active bacteria that display antagonistic but complementary behavior. While the inner core provides a chemically powered light source, the outer shell works as a visual sensor for a specific chemical that activates the biological machinery of the engineered cells. Because of the precise localization of the two strains, it was possible to harness their functionalities and to use the 3D-printed objects for a proof-of-concept application as a living sensing device.

3. Conclusions

Light-based printing of hydrogels loaded with microorganisms is an effective approach to generate complex living materials with multiple bacteria and exquisite 3D shapes. Hydrogel inks containing methacrylated copolymer and hyaluronic acid were found to display rheological properties that are suitable for both DLP and VP techniques. The biocompatible nature of these photoactive species allows for the incorporation of wild-type and genetically engineered bacteria into the hydrogel ink. Despite the confining viscoelastic nature of the printed hydrogels, the embedded microorganisms are able to grow and form metabolically active colonies when immersed for several days in culture medium. The shaping freedom offered by light-based printing enables the creation of bacteria-laden materials with complex morphologies and functionalities that are very distinct from those encountered in nature. Using bioluminescent and melanin-producing engineered bacteria, living objects can be genetically programmed to change color in response to specific chemical species, thus creating a chemically powered sensor with a simple visual readout. The vast range of biochemical pathways accessible in wild or engineered bacteria combined with the free-shaping capabilities of light-based printing opens new possibilities for the synthesis of bacteria-driven complex materials with unique metabolic and living functionalities.

4. Experimental Section

Materials: Sodium hyaluronate (95%) was purchased from Acros Organics and used as received. Methacrylic anhydride (94%), Pluronic F-127, triethylamine, LAP (≥ 95%), diethyl ether (≥ 99.8%), hydrochloric acid (37%), sodium hydroxide (98–100.5%), quinoline yellow, copper(II) sulfate pentahydrate, kanamycin sulfate (K1377), Photobacterium Broth and Marine Broth 2216 were purchased from Sigma-Aldrich and used as received. LB Miller media was made using LB broth (low salt, L3397) and sodium chloride (to a final concentration 10 g L^{-1}), both purchased from Sigma-Aldrich. Milli-Q water was obtained from a Nanopure Diamond Lab Water System from Barnstead with a resistivity of 18.2 MΩ cm. Phosphate buffered saline (PBS, pH 7.4, 10010015) was obtained from ThermoFisher Scientific. Low melt agarose (BIA1189), isopropyl-beta-D-thiogalactopyranoside (IPTG, BIMB1008), and L-tyrosine (>95%, BIT0721) were obtained from Apollo Scientific. DNA synthesis was performed by Integrated DNA Technologies (IDT). Bacterial strains used were *Photobacterium kishitanii* 201212X for bioluminescence, *E. coli* DH5α (ThermoFisher) for cloning, and *E. coli* sAJM.1505 was used for AIDA-Tyr1 expression since it is a Δ*ompT* strain, required for AIDA-based display.

Modification of Hyaluronic Acid and Pluronic F-127: The reaction to synthesize HAMA was performed in a 250 mL round-bottom flask, following a previously reported protocol.[3] Briefly, 1 equivalent of sodium hyaluronate was dissolved overnight in 100 mL Milli-Q water and the solution was brought to pH 8 by dropwise addition of 1 M NaOH. The solution was then transferred on an ice bath and 20 equivalents of methacrylic anhydride were added under vigorous stirring. The pH of the solution was maintained at 8 by dropwise addition of NaOH for 3 h, after which the solution was maintained overnight at 5 °C under stirring. The product was then collected by precipitation into ice-cold ethanol, dissolved in Milli-Q water, and transferred into dialysis tubes (VWR, cut off 12–14 kDa) before dialysis against Milli-Q water for 5 days. Finally, the purified HAMA was freeze-dried to obtain a cotton-like powder that was stored at −20 °C. Successful modification was confirmed by the detection of methacrylate peaks in ^{1}H NMR, after dissolution of the product in deuterated water.

To synthesize Pluronic dimethacrylate (PluDMA), a previously reported protocol was followed.[27] Initially, Pluronic F-127 was dried overnight at 40 °C and 10 mbar. Later, 1 equivalent of the dried polymer was added in a 250 mL round-bottom flask and dissolved in 100 mL of $CHCl_3$. The solution was then placed on an ice bath and 8 equivalents of triethylamine (TEA) were added to the reaction vessel. After complete dissolution, 8 equivalents of methacrylic anhydride were added under vigorous stirring. The flask was then flushed with dry nitrogen for 2 min and sealed with a septum. An argon-filled balloon was mounted in the septum via a needle. The reaction was kept in ice for the first 8 h and then allowed to proceed at room temperature for 16 additional h. Afterward, the PluDMA was precipitated in cold diethyl ether and collected using a Büchner funnel. The wet precipitate was then dried at 10 mbar overnight. The product was dissolved in $CHCl_3$ and added in a 1:10 volume ratio to centrifuge tubes filled with cold diethyl ether. After centrifugation at 3350 rcf, the liquid was decanted from the tubes and the PluDMA was dried at 10 mbar overnight. The resulting off-white powder was stored at −20 °C. To confirm methacrylation of the chain ends, ^{1}H NMR was performed after dissolution of the product in DMSO-d_6.

DLP Printing: All samples printed using DLP were produced with an Ember DLP printer (Autodesk), equipped with a 405 nm lamp able to provide 22 mW cm^{-2} at maximum intensity. The ink for DLP prints was prepared by initially dissolving 1% w/v HAMA and 20% w/v PluDMA in Milli-Q water. After the pH of the solution was adjusted to 6 using 1 M NaOH, 0.018% w/v quinoline yellow and 0.5% w/v LAP were added to complete the ink. In the while, an inoculum of *P. kishitanii* was prepared in Marine Broth 2216 starting from a −80 °C stock solution and was added to the ink at a 1:100 dilution. To maintain the density of the bacteria constant, the inoculum was used after the absorbance measured at 600 nm reached a value of 0.1.

For printing, the ink was printed in 100 µm thick layers using 1 s exposure time per layer. After printing, the structures were first rinsed and then stored under stirring in fresh Marine Broth 2216.

VP: All samples printed using VP were produced with a Tomolite (Readily 3D) volumetric printer, using Pyrex glass vials having an internal diameter of 14.4 mm. The ink for VP prints was prepared by initially dissolving 1% w/v HAMA and 20% w/v PluDMA in Milli-Q water. Later, the pH of the solution was adjusted to 6 using 1 M NaOH. To complete the ink, 0.05% w/v LAP was added to the solution prior to printing.

When loading the ink with *P. kishitanii*, it was proceeded as described in the case of DLP prints. To load the ink with engineered *E. coli*, a selective streak plate from a –80 °C stock solution was prepared first. A colony was then collected from the plate using a loop and suspended in LB media with 50 µg mL^{-1} kanamycin. The resulting inoculum was used when the absorbance measured at 600 nm reached a value of 0.2 and was added to the ink at a 1:100 dilution.

After loading the ink in the printing vial, the prints were performed at a light dose of 120 mJ cm^{-2}. Due to the lack of a photoblocker in the composition, care was taken not to expose the ink to light, thus preventing possible pre-curing of the material. For consecutive prints, the printed shell was first washed in media to ensure no uncured material was present. Then, the shell was placed in a clean vial, which was then filled with new ink. The print within the object was executed at 140 mJ cm^{-2} to ensure full curing of the core. The completed device was then rinsed and placed in fresh culture media.

Imaging: To macroscopically image the prints, photographs were taken using a Canon EOS 6D reflex camera equipped with a Macro 100 mm objective at different exposure times. For visualizing bioluminescence, pictures were taken in a dark room with an exposure time of 6 s. To identify the regions with different strains in the dual-bacteria devices, images taken in the dark were overlapped with the ones taken with regular lighting using the image processing software Fiji.[28]

The growth of colonies within the prints was microscopically imaged using a confocal microscope (SP8 Lightning, Leica microsystems) in bright-field mode.

Optical Measurements: Bioluminescence and absorbance spectra were recorded using a Varioskan LUX plate reader (Thermo Scientific). Bacterial cultures for inoculation were grown shaken in 10 mL of their respective media in a 50 mL tube, and their absorbance at 600 nm was regularly measured in a 200 µL aliquot in a 96-well plate. Thus, for *E. coli*, an absorbance at 600 nm reading of 0.1 corresponded to OD600 of ≈0.2, and a bacterial density of 3×10^7 cells mL^{-1}.[29] Prints were measured after being positioned in 24-well plates. Bioluminescence spectra were recorded between 450 and 550 nm, and the maxima were used to quantify the luminescence of the prints. Absorbance spectra were recorded between 300 and 800 nm. To quantify the effect of melanin on the absorbance spectra and tell it apart from the increase in turbidity due to bacterial growth, the difference between the absorbance value at 400 nm and that at 800 nm (A400 – A800) was taken as the measure of darkening.

The colorimetric evaluation of the scaffolds was performed on photographs taken in a fixed lighting set. Using Fiji,[28] RGB spectra and HEX color values were extracted from the pixels belonging to the prints.

Plasmid Design and Construction: Plasmid pLN-AIDA-Tyr1 was based on the backbone of plasmid pL6FO,[30] which contained a low copy number pSC101 origin and kanamycin resistance, as well as constitutively expressed LacI. The AIDA-Tyr1 sequence was taken from the literature,[31] and the AIDA sequence was amplified from pAIDA1 (Addgene #79180) and the Tyr1 gene fragment was synthesized as a gBlock (IDT). A detailed description of the plasmid optimization process and the gene sequences can be found in Methods in the Supporting Information. pLN-AIDA-Tyr1 DNA and full sequence information is also available from Addgene, plasmid #192831.

DNA construction was performed by Gibson assembly,[32] following the protocol in reference using enzymes Taq ligase (M0208S), T5 Exonuclease (M0663S), and Phusion polymerase (M0530S), obtained from New England Biolabs (NEB). Polymerase chain reaction (PCR) fragments were obtained with custom DNA oligos and Q5 Hot Start High-Fidelity (M0494L) was also obtained from NEB. PCR fragments were purified with Reliaprep DNA Clean-Up and concentration system (A2892, Promega). Cloning was performed in *E. coli* DH5a chemically competent cells. Plasmid purification was performed with PureYield Plasmid Minipreps System (A1223, Promega). DNA sequence was confirmed by Sanger sequencing carried out by MicroSynth.

Melanin Quantification: To quantify melanin production by engineered *E. coli* in a hydrogel environment, 2x LB Miller media was made and combined 1:1 with a solution of 1.5% w/v low melt agarose, supplemented with 1 g L^{-1} L-tyrosine, 16×10^{-6} M $CuSO_4$, 50 µg mL^{-1} kanamycin, and varying concentrations of IPTG. This medium was kept warm in a water bath at 40 °C, then inoculated with *E. coli* and dispensed into 24-well plates (92424, TPP) at 1 mL per well. The inoculating *E. coli* were first grown overnight in LB Miller medium with 50 µg mL^{-1} kanamycin, and diluted 1:1000 into fresh media. The resulting 0.75% agarose gels were left to set at room temperature for an hour, before being placed into a static 37 °C incubator. The absorbance spectrum of each well was then measured in a plate reader.

To extract melanin pigment, cells were streaked out onto 1.5% agar plates with LB Miller medium, supplemented with 1 g L^{-1} L-tyrosine, 16×10^{-6} M $CuSO_4$, 50 µg mL^{-1} kanamycin, and 0.2×10^{-3} M IPTG. After 5 days of incubation at 37 °C, the dark 25 mL agar gel was removed from the plate and added to 250 mL PBS and left shaking overnight at room temperature. This resulted in a dark brown solution, which was sterile filtered through a 0.22 µm membrane (99250, TPP) to remove bacteria, and the resulting liquid was assessed in the plate reader, alongside PBS controls which were used as a background value.

Rheological Testing: Rheological measurements were performed with an MCR 302 compact rheometer (Anton Paar). A PP25-S geometry was used for recording flow curves, whereas a glass PP43 geometry was utilized for oscillatory measurements and for testing the curing behavior. All measurements were performed at 25 °C. Flow curves were recorded during rotational strain-controlled measurements with a shear rate ramping linearly from 0.1 to 100 s^{-1}. For the analysis of the storage modulus (G') of the inks and of the curing timescale, oscillatory measurements were performed at 1% deformation and 1 rad s^{-1} frequency over time. After 55 s, an intense LED light at 385 nm was shone on the sample to trigger photocrosslinking. The characteristic photocrosslinking timescale τ for each ink composition was calculated by fitting the data using the exponential expression $G' = G'_{max}(1 - e^{-t/\tau})$.

Statistical Analysis: The experimental data displayed in Figures 1–4 and Figures S1–S5 in the Supporting Information were processed using Microsoft Excel and Plot2. No statistical analysis was performed for the data obtained using the Varioskan LUX Plate Reader and the Canon EOS 6D digital camera. The flow curves of different ink formulations shown in Figure 1 were fitted using the Carreau model with the Anton Paar RheoCompass software to obtain the displayed values of zero-shear viscosity. The analysis of the colony size evolution was performed using the *Analyze Particles* plugin included in Fiji[28] to obtain a distribution of the cross-sectional area of the growing *P. kishitanii* colonies. Prior to the measurement, the images were binarized and noise was reduced by removing objects smaller than 5 µm and with a circularity lesser than 0.7 from the count. The NMR spectra shown in Figure S1 in the Supporting Information were processed with Mnova and Plot2. A baseline correction using a Bernstein Polynomial Fit for the baseline was performed to improve the visualization of the peaks.

Supporting Information

Supporting Information is available from the Wiley Online Library or from the author.

Acknowledgements

The authors thank the Strategic Focus Area Advanced Manufacturing (SFA-AM) of the Swiss ETH domain for financially supporting this

research as part of the D-SENSE project. The research also benefitted from support from the Swiss National Science Foundation within the framework of the National Center of Competence in Research for Bio-Inspired Materials. The authors thank Prof. Dr. Marcy Zenobi-Wong for kindly providing access to the Tomolite volumetric printer and Riccardo Rizzo for the introduction to the setup. The authors thank Stefano Menasce for his support in the acquisition and analysis of NMR spectra. Prof. Henryk Urbanczyk (University of Miyazaki) is also greatly acknowledged for the kind supply of the bioluminescent bacteria *P. kishitanii*. *E. coli* sAJM.1505 was a gift from Christopher Voigt (Addgene #108253). pAIDA1 was a gift from Gen Larsson (Addgene plasmid #79180).

Conflict of Interest

The authors declare no conflict of interest.

Data Availability Statement

The data that support the findings of this study are available from the corresponding author upon reasonable request.

Keywords

DLP printing, engineered living materials, printed living materials, volumetric printing

Received: August 17, 2022
Revised: November 23, 2022
Published online: December 18, 2022

[1] a) P. Q. Nguyen, N. M. D. Courchesne, A. Duraj-Thatte, P. Praveschotinunt, N. S. Joshi, *Adv. Mater.* **2018**, *30*, 1704847; b) X. Liu, H. Yuk, S. Lin, G. A. Parada, T.-C. Tang, E. Tham, C. de la Fuente-Nunez, T. K. Lu, X. Zhao, *Adv. Mater.* **2018**, *30*, 1704821; c) A. Rodrigo-Navarro, S. Sankaran, M. J. Dalby, A. del Campo, M. Salmeron-Sanchez, *Nat. Rev. Mater.* **2021**, *6*, 1175.

[2] A. M. Duraj-Thatte, N. M. D. Courchesne, P. Praveschotinunt, J. Rutledge, Y. Lee, J. M. Karp, N. S. Joshi, *Adv. Mater.* **2019**, *31*, 1901826.

[3] M. Schaffner, P. A. Ruhs, F. Coulter, S. Kilcher, A. R. Studart, *Sci. Adv.* **2017**, *3*, eaao6804.

[4] S. Sankaran, S. Zhao, C. Muth, J. Paez, A. del Campo, *Adv. Sci.* **2018**, *5*, 1800383.

[5] a) H. M. Jonkers, in *Self-Healing Materials: An Alternative Approach to 20 Centuries of Materials Science*, (Ed: S. van derZwaag), Springer Netherlands, Dordrecht **2007**, p. 195; b) H. M. Jonkers, A. Thijssen, G. Muyzer, O. Copuroglu, E. Schlangen, *Ecol. Eng.* **2010**, *36*, 230; c) C. M. Heveran, S. L. Williams, J. Qiu, J. Artier, M. H. Hubler, S. M. Cook, J. C. Cameron, W. V. Srubar, *Matter* **2020**, *2*, 481; d) H. W. Kua, S. Gupta, A. N. Aday, W. V. Srubar, *Cem. Concr. Compos.* **2019**, *100*, 35.

[6] S. Gantenbein, E. Colucci, J. Käch, E. Trachsel, F. B. Coulter, P. A. Rühs, K. Masania, A. R. Studart, eprint, arXiv:2203.00976, **2022**.

[7] a) L. J. Bird, E. L. Onderko, D. A. Phillips, R. L. Mickol, A. P. Malanoski, M. D. Yates, B. J. Eddie, S. M. Glaven, *MRS Commun.* **2019**, *9*, 505; b) S. Molinari, R. F. Tesoriero, D. Li, S. Sridhar, R. Cai, J. Soman, K. R. Ryan, P. D. Ashby, C. M. Ajo-Franklin, *Nat. Commun.* **2022**, *13*, 5544; c) C.-P. Tseng, F. Liu, X. Zhang, P.-C. Huang, I. Campbell, Y. Li, J. T. Atkinson, T. Terlier, C. M. Ajo-Franklin, J. J. Silberg, R. Verduzco, *Adv. Mater.* **2022**, *34*, 2109442; d) L. J. Bird, B. B. Kundu, T. Tschirhart, A. D. Corts, L. Su, J. A. Gralnick, C. M. Ajo-Franklin, S. M. Glaven, *ACS Synth. Biol.* **2021**, *10*, 2808; e) X. Liu, Y. Yang, M. E. Inda, S. Lin, J. Wu, Y. Kim, X. Chen, D. Ma, T. K. Lu, X. Zhao, *Adv. Funct. Mater.* **2021**, *31*, 2010918.

[8] a) G. O'Toole, H. B. Kaplan, R. Kolter, *Annu. Rev. Microbiol.* **2000**, *54*, 49; b) N. Lane, *The Vital Question: Energy, Evolution, and the Origins of Complex Life*, W. W. Norton, New York **2015**.

[9] P. Fratzl, R. Weinkamer, *Prog. Mater. Sci.* **2007**, *52*, 1263.

[10] a) M. Rafiee, R. D. Farahani, D. Therriault, *Adv. Sci.* **2020**, *7*, 1902307; b) S. Park, W. Shou, L. Makatura, W. Matusik, K. Fu, *Matter* **2022**, *5*, 43.

[11] a) S. V. Murphy, A. Atala, *Nat. Biotechnol.* **2014**, *32*, 773; b) J. M. Unagolla, A. C. Jayasuriya, *Appl. Mater. Today* **2020**, *18*, 100479; c) R. Levato, T. Jungst, R. G. Scheuring, T. Blunk, J. Groll, J. Malda, *Adv. Mater.* **2020**, *32*, 1906423; d) I. Matai, G. Kaur, A. Seyedsalehi, A. McClinton, C. T. Laurencin, *Biomaterials* **2020**, *226*, 119536.

[12] A. Saha, T. G. Johnston, R. T. Shafranek, C. J. Goodman, J. G. Zalatan, D. W. Storti, M. A. Ganter, A. Nelson, *ACS Appl. Mater. Interfaces* **2018**, *10*, 13373.

[13] a) B. A. E. Lehner, D. T. Schmieden, A. S. Meyer, *ACS Synth. Biol.* **2017**, *6*, 1124; b) D. T. Schmieden, S. J. Basalo Vázquez, H. Sangüesa, M. van der Does, T. Idema, A. S. Meyer, *ACS Synth. Biol.* **2018**, *7*, 1328.

[14] J. Zhang, Q. Hu, S. Wang, J. Tao, M. Gou, *Int. J. Bioprint.* **2020**, *6*, 19.

[15] J. C. Ast, I. Cleenwerck, K. Engelbeen, H. Urbanczyk, F. L. Thompson, P. De Vos, P. V. Dunlap, *Int. J. Syst. Evol. Microbiol.* **2007**, *57*, 2073.

[16] a) Y. Shen, H. Tang, X. Huang, R. Hang, X. Zhang, Y. Wang, X. Yao, *Carbohydr. Polym.* **2020**, *235*, 115970; b) S. H. Kim, Y. K. Yeon, J. M. Lee, J. R. Chao, Y. J. Lee, Y. B. Seo, M. T. Sultan, O. J. Lee, J. S. Lee, S.-I. Yoon, I.-S. Hong, G. Khang, S. J. Lee, J. J. Yoo, C. H. Park, *Nat. Commun.* **2018**, *9*, 1620; c) P. Kunwar, A. V. S. Jannini, Z. Xiong, M. J. Ransbottom, J. S. Perkins, J. H. Henderson, J. M. Hasenwinkel, P. Soman, *ACS Appl. Mater. Interfaces* **2020**, *12*, 1640; d) M. Pagac, J. Hajnys, Q.-P. Ma, L. Jancar, J. Jansa, P. Stefek, J. Mesicek, *Polymers* **2021**, *13*, 598.

[17] a) P. N. Bernal, P. Delrot, D. Loterie, Y. Li, J. Malda, C. Moser, R. Levato, *Adv. Mater.* **2019**, *31*, 1904209; b) R. Rizzo, D. Ruetsche, H. Liu, M. Zenobi-Wong, *Adv. Mater.* **2021**, *33*, 2102900.

[18] D. Loterie, P. Delrot, C. Moser, *Nat. Commun.* **2020**, *11*, 852.

[19] P. V. Dunlap, H. Urbanczyk, in *The Prokaryotes: Prokaryotic Physiology and Biochemistry*, (Eds: E. Rosenberg, E. F. DeLong, S. Lory, E. Stackebrandt, F. Thompson), Springer Berlin Heidelberg, Berlin, Heidelberg **2013**, pp. 495.

[20] S. Bhusari, S. Sankaran, A. del Campo, *Adv. Sci.* **2022**, *9*, 2106026.

[21] S. Torquato, S. Hyun, A. Donev, *Phys. Rev. Lett.* **2002**, *89*, 266601.

[22] S. C. Kapfer, S. T. Hyde, K. Mecke, C. H. Arns, G. E. Schröder-Turk, *Biomaterials* **2011**, *32*, 6875.

[23] G. M. Casanola-Martin, H. Le-Thi-Thu, Y. Marrero-Ponce, J. A. Castillo-Garit, F. Torrens, A. Rescigno, C. Abad, M. T. Khan, *Curr. Top. Med. Chem.* **2014**, *14*, 1494.

[24] M. Gustavsson, D. Hörnström, S. Lundh, J. Belotserkovsky, G. Larsson, *Sci. Rep.* **2016**, *6*, 36117.

[25] R. Lutz, H. Bujard, *Nucleic Acids Res.* **1997**, *25*, 1203.

[26] G. Zonios, A. Dimou, I. Bassukas, D. Galaris, A. Tsolakidis, E. Kaxiras, *J. Biomed. Opt.* **2008**, *13*, 014017.

[27] K.-H. Hong, Y.-S. Jeon, J.-H. Kim, *Macromol. Res.* **2009**, *17*, 26.

[28] J. Schindelin, I. Arganda-Carreras, E. Frise, V. Kaynig, M. Longair, T. Pietzsch, S. Preibisch, C. Rueden, S. Saalfeld, B. Schmid, J.-Y. Tinevez, D. J. White, V. Hartenstein, K. Eliceiri, P. Tomancak, A. Cardona, *Nat. Methods* **2012**, *9*, 676.
[29] G. Sezonov, D. Joseleau-Petit, R. D'Ari, *J. Bacteriol.* **2007**, *189*, 8746.
[30] A. Kan, D. P. Birnbaum, P. Praveschotinunt, N. S. Joshi, *Appl. Environ. Microbiol.* **2019**, *85*, e00434.
[31] D. Hörnström, G. Larsson, A. J. A. van Maris, M. Gustavsson, *Biochim. Biophys. Acta, Biomembr.* **2019**, *1861*, 486.
[32] D. G. Gibson, L. Young, R. Y. Chuang, J. C. Venter, C. A. Hutchison3rd, H. O. Smith, *Nat. Methods* **2009**, *6*, 343.